



Experimental production of charcoal morphologies to discriminate fuel source and fire type: an example from Siberian taiga

Angelica Feurdean

Department of Physical Geography, Goethe University, Altenhöferallee 1, 60438 Frankfurt am Main, Germany

Correspondence: Angelica Feurdean (angelica.feurdean@gmail.com, feurdean@em.uni-frankfurt.de)

Received: 14 January 2021 – Discussion started: 1 February 2021

Revised: 28 May 2021 – Accepted: 30 May 2021 – Published:

Abstract. The analysis of charcoal fragments in peat and lake sediments is the most widely used approach to reconstruct past biomass burning. With a few exceptions, this method typically relies on the quantification of the total charcoal content of the sediment. To enhance charcoal analyses for the reconstruction of past fire regimes and make the method more relevant to studies of both plant evolution and fire management, the extraction of more information from charcoal particles is critical. Here, I used a muffle oven to burn seven fuel types comprising 17 species from boreal Siberia (near Teguldet village), which are also commonly found in the Northern Hemisphere, and built on published schemes to develop morphometric and finer diagnostic classifications of the experimentally charred particles. I then combined these results with those from fossil charcoal from a peat core taken from the same location (Ulukh-Chayakh mire) in order to demonstrate the relevance of these experiments to the fossil charcoal records. Results show that graminoids, *Sphagnum*, and wood (trunk) lose the most mass at low burn temperatures ($< 300^{\circ}\text{C}$), whereas heathland shrub leaves, brown moss, and ferns lose the most mass at high burn temperatures. This suggests that species with low mass retention in high-temperature fires are likely to be under-represented in the fossil charcoal record. The charcoal particle aspect ratio appeared to be the strongest indicator of the fuel type burnt. Graminoid charcoal particles are the most elongate (6.7–11.5), with a threshold above 6 that may be indicative of wetland graminoids; leaves are the shortest and bulkiest (2.1–3.5); and twigs and wood are intermediate (2.0–5.2). Further, the use of fine diagnostic features was more successful in separating wood, graminoids, and leaves, but it was difficult to further differentiate these fuel types due to overlapping features. High-aspect-ratio particles, dominated

by graminoid and *Sphagnum* morphologies, may be robust indicators of low-temperature surface fires, whereas abundant wood and leaf morphologies as well as low-aspect-ratio particles are indicative of higher-temperature fires. However, the overlapping morphologies of leaves and wood from trees and shrubs make it hard to distinguish between high-intensity surface fires, combusting living shrubs and dead wood and leaves, and high-intensity crown fires that have burnt living trees. Distinct particle shape may also influence charcoal transportation, with elongated particles (graminoids) potentially having a more heterogeneous distribution and being deposited farther away from the origin of fire than the rounder, polygonal leaf particles. Despite these limitations, the combined use of charred-particle aspect ratios and fuel morphotypes can aid in the more robust interpretation of fuel source and fire-type changes. Lastly, I highlight the further investigations needed to refine the histories of past wildfires.

1 Introduction

Wildfires are the most common disturbance type in boreal forests, triggering gap dynamics or stand-scale forest replacement depending on intensity (temperature of fire) and frequency (Goldammer and Furayev, 1996). Ongoing and anticipated increases in the intensity and frequency of wildfire in boreal forests is raising concerns about its impact on forest composition as well as climate (Jones et al., 2020). Although the largest area of boreal forest globally is in Siberia (Goldammer and Furayev, 1996), its extent and access restrictions mean there are only a few datasets recording changes in wildfire activity, especially from a longer-term perspective (Marlon et al., 2016). Long-term records of wild-

fire activity are vital to understanding how fire regimes vary with changes in climate and human–vegetation interaction, as well as the impacts of fires on boreal forests.

Wildfires can reach temperatures of up to 1800 °C. Charcoal, however, is an inorganic carbon compound resulting from the incomplete combustion of plant tissues, which typically occurs at temperatures between 280 and 500 °C (Rein, 2014). Charcoal particles vary with respect to size and form, and characteristics, such as edge aspects, surface features, cleavage, lustre, or anatomical details (e.g. tracheids with border pits, leaf veins, and cuticles), that can be used to determine their origin are often preserved (Ward and Hardy, 1991; MacDonald et al., 1991; Scott, 2010; Enache and Cumming, 2006; Jensen et al., 2007; Courtney-Mustaphi and Pisaric, 2014a; Hubau et al., 2012, 2013; Prince et al., 2018). Although macroscopic charcoal analysis, typically counting charcoal pieces or charcoal area per unit sediment volume from a small sediment volume (1–2 cm³), is widely done, there has been less focus on the reconstruction of fuel sources. However, fuel-type identification is a crucial factor in determining fire type (i.e. the burning of surface fuels in low- or high-intensity fires) or distinguishing between surface and crown fires (CE1). At a minimum, this requires a better characterisation of charcoal morphology to indicate the nature of the plant material burnt (Courtney-Mustaphi and Pisaric, 2014a, b; Feurdean et al., 2017; Hawthorne et al., 2018). The determination of fire type is not only helpful for palaeo-fire reconstructions but could also provide an accessible tool for ecosystem managers and modellers as well as for assessing and mitigating the risks of fires that might impact settlements and infrastructures (Moritz et al., 2014).

Ongoing efforts have advanced the utility of charcoal morphological analyses for fuel-type identification and fire regime reconstruction. Umbanhowar and McGrath (1998), Crawford and Belcher (2014), and Pereboom et al. (2020) conducted morphometric measurements of the length, aspect ratio (length / width), and surface area of charcoal particles by burning known plant materials originating from American prairie, tropical, and Arctic environments in the laboratory. They concluded that longer fragments correspond to graminoids, whereas shorter fragments originate from wood, shrubs, and leaves. Nichols et al. (2000) and Crawford and Belcher (2014) additionally found that charcoal morphometry is generally preserved during transportation by water. Other studies have focused on the effects of burning conditions, i.e. open-flame ignition, muffle furnace experiments (Umbanhowar and McGrath, 1998; Orvis et al., 2005), and combustion calorimetry (Hudspith et al., 2018), on charcoal production. In a laboratory study, Belcher et al. (2005, 2015) investigated whether fire can be ignited by thermal radiation and may have been the reason for major extinction events in deep geological times, with results giving little support for this hypothesis. Jensen et al. (2007) and Courtney-Mustaphi and Pisaric (2014a) examined subtler diagnostic features (morphology, surface features, lustre) of laboratory-

produced charcoal morphotypes of a small number of North American grasses and leaves of coniferous and deciduous trees. Enache and Cumming (2006, 2007) and Mustaphi and Pisaric (2014a) classified charcoal morphologies in Canadian lake sediments based on particle shape, aspect ratio, and surface features, and linked these morphometric characteristics to fuel types. Courtney-Mustaphi and Pisaric (2014a) also discussed the potential for categorising charcoal morphologies to explore relationships with taphonomic processes and fuel types. A number of recent studies have attributed fossil charred particles to specific fuel and fire types based on published morphotype categorisations (Walsh et al., 2008; Daniau et al., 2013; Aleman et al., 2013; Leys et al., 2015; Courtney-Mustaphi and Pisaric, 2014a, b, 2018; Feurdean et al., 2017, 2019, 2020; Feurdean and Vasiliev, 2019; Unkelbach et al., 2018).

This paper presents the first results of laboratory-produced (muffle oven) charcoal morphologies spanning a range of fuel types from 17 Siberian species, with the aim of characterising the diversity of charcoal morphologies produced by boreal understorey and forest vegetation to facilitate more robust interpretations of fuel sources from this region. Specifically, this work (i) evaluates whether there are morphological distinctions (morphometrics and finer anatomical features) between species or fuel types, and (ii) explores the effect of burning temperature on the mass, morphometrics, and finer anatomical features of charred plant material. This combination of factors has not been widely tested in the laboratory, so this study has the potential to advance our understanding of the link between sedimentary charcoal morphologies and fire types and, as the species occur across most of the Northern Hemisphere, refine wildfire histories in boreal regions.

2 Material and methods

2.1 Laboratory analysis

Plant materials used for laboratory burning experiments were identified in the field, stored in plastic bags for transportation, and air-dried. Selected materials include a range of fuel types (graminoid, trunk wood, twigs from trees and shrubs, leaves from coniferous and deciduous trees, shrubs, forbs, and ferns, and fern and moss stems with leaves) from the most common tree, shrub, herb, fern, and moss species around a forested mire near Teguldet village, Tomsk district, Russia. This light boreal taiga forest is primarily composed of *Pinus* and *Betula*. Additionally, needles and twigs of *Picea abies* were collected from Taunus, near Frankfurt am Main, Germany (Table 1). All plant material was collected from living plants, except trunk wood, which was taken from a dead tree.

To determine the mass, morphometrics, and finer diagnostic features of residual charred plant material as well the effect of increasing temperatures on all these characteristics, the dried remains of individual plant species were placed in

Table 1. List of plant materials burned. All plants are from Siberia except for *Picea abies*, which originated in Taunus, Germany. All plant material was air-dried before combustion in the muffle oven. Leaves of deciduous trees and shrubs include veins and petioles. The term “twig” was only used for woody species (i.e. deciduous and coniferous trees and shrubs), and no distinction was made between soft young wood.

Plant type	Scientific name	Family	Common name	Plant burned
Trees				
Conifer tree	<i>Pinus sylvestris</i>	Pinaceae	Scots pine	Needles
Conifer tree	<i>Pinus sylvestris</i>	Pinaceae	Scots pine	Twigs
Conifer tree	<i>Pinus sylvestris</i>	Pinaceae	Scots pine	Dead wood
Conifer tree	<i>Pinus sibirica</i>	Pinaceae	Siberian pine	Needles
Conifer tree	<i>Pinus sibirica</i>	Pinaceae	Siberian pine	Twigs
Conifer tree	<i>Picea abies</i>	Pinaceae	Norway spruce	Needles
Conifer tree	<i>Picea abies</i>	Pinaceae	Norway spruce	Twigs
Deciduous tree	<i>Betula pendula</i>	Betulaceae	Silver birch	Leaves
Deciduous tree	<i>Betula pendula</i>	Betulaceae	Silver birch	Twigs
Shrubs				
Shrub	<i>Vaccinium myrtillus</i>	Ericaceae	Bilberry	Leaves
Shrub	<i>Vaccinium myrtillus</i>	Ericaceae	Bilberry	Twigs
Shrub	<i>Oxycoccus palustre</i>	Ericaceae	Cranberry	Leaves
Shrub	<i>Oxycoccus palustre</i>	Ericaceae	Cranberry	Twigs
Shrub	<i>Empetrum nigrum</i>	Ericaceae	Crowberry	Leaves
Shrub	<i>Empetrum nigrum</i>	Ericaceae	Crowberry	Twigs
Shrub	<i>Ledum palustre</i>	Ericaceae	Wild rosemary	Leaves
Shrub	<i>Ledum palustre</i>	Ericaceae	Wild rosemary	Twigs
Shrub	<i>Chamaedaphne calyculata</i>	Ericaceae	Leatherleaf	Leaves
Shrub	<i>Chamaedaphne calyculata</i>	Ericaceae	Leatherleaf	Twigs
Herbaceous				
Graminoid	<i>Eriophorum vaginatum</i>	Cyperaceae	Cotton grass	Leaves
Graminoid	<i>Calamagrostis</i>	Poaceae	Reed grass	Leaves
Graminoid	<i>Carex</i> spp.	Cyperaceae	Sedge	Leaves
Forb	<i>Cnidium dubium</i>	Apiaceae	Leaves	
Forb	<i>Rubus</i> spp.	Rosaceae	Raspberry	Leaves
Fern	<i>Polypodium</i>	Polypodiaceae	Fern	Leaves
Fern	<i>Equisetum palustre</i>	Equisetaceae	Horsetail	Stem
Moss	<i>Sphagnum</i> spp.	Sphagnaceae	Peat moss	Stem and leaves
Moss	<i>Polytrichum commune</i>	Politrachaceae	Hair moss	Stem and leaves

ceramic crucibles, weighed, covered with a lid to limit oxygen availability and avoid mixing of the charred particles, and heated for 2 h in a muffle oven (preheated for 1 h); they were then roasted at 250, 300, 350, 400, or 450 °C (File S1 in the Supplement). No burning experiments were conducted at higher temperatures because all plant material turned to ash, i.e. a solid residue mostly composed of minerals that crumbled apart into soot and fly ash (Rein et al., 2014). The effect of mixing plant material in known ratios on charred mass and morphometrics at an intermediate temperature (300 °C) was also tested. For this experiment, the plant material was combined in volumes to approximate the predominant fuel mixtures for low-intensity surface fires (with a ratio of 75 % graminoid and moss to 25 % shrub, and 50 % graminoid to 50 % moss and fern), intermediate- to high-intensity surface

fires (with a ratio of 25 % graminoid and moss to 75 % shrub, and 50 % graminoid and moss to 50 % shrub), and high-intensity crown fires (with a ratio of 50 % graminoid, shrub, and moss to 50 % wood and leaf). The experimental temperatures were chosen based on the range of temperatures reported in the literature (250–500 °C; Umbanhowar and McGrath, 1998; Orvis et al., 2005; Jensen et al., 2007; Pereboom et al., 2020). Although dry roasting in a muffle oven approximates some aspects of the heating conditions of vegetation in a natural fire, it does not explore the impact of how long the material was at specific burning temperature and oxygen conditions (Belcher et al., 2015; Hudspith et al., 2018). Dry roasting also reduces the influence of flame dynamics and turbulent airflow; therefore, plant tissue is more rapidly reduced to ash than in natural fires. After cooling, the remain-

ing charred mass of each sample was weighed and the ratio of charred to pre-combustion mass was calculated. Charred samples were then split into two subsets. The first was left intact and stored as reference material. The second subsample was gently disaggregated with a mortar and pestle to mimic the natural breakage that charcoal particles incur over time in sediment (Umbanhowar and McGrath, 1998; Crawford and Belcher, 2014; Belcher et al., 2015) and was then washed through a 125 μm sieve to remove smaller fragments. This second subsample was used to make morphometric measurements and to characterise finer diagnostic features. Morphometric measurements of individual charred particles were obtained from photographs taken at 4 \times magnification with a digital camera (KERN ODC 241 tablet camera). On average, more than 100 charcoal particles larger than 150 μm were automatically detected in most samples, except for those burnt at higher temperatures, where particles were more prone to breaking up. The major (L) and minor (W) axes, along with surface area (A) of each particle were measured following the algorithm given in Appendix A1, and the aspect ratio L/W was calculated. Finer diagnostic features such as shape, surface features (e.g. reticulates, tracheids with border pits, leaf veins, the arrangement of epidermal cells, and cuticles with stomata), and cleavage were characterised at 4 \times magnification by inspection of microphotographs or observations of the charred particles themselves under a microscope or stereomicroscope.

To demonstrate the applicability of these experiments to fossil records, seven samples with high charcoal content were selected from a sediment core from Ulukh-Chayakh mire near Teguldet village (Feurdean et al., 2021). Sample preparation followed Feurdean et al. (2020) and included bleaching overnight and washing in a 150 μm sieve. The results were compared to pollen and plant macrofossils data from the same core.

2.2 Numerical analysis

The medians and standard deviations of charcoal morphometrics (L , L/W , and A) were aggregated for each species, fuel type, and burn temperature, and are displayed as box plots. A two-tailed Mann–Whitney test was used to test whether the medians of the charcoal morphometrics of various fuel types were equal (File S2). This test does not assume a normal distribution, only similar distributions in both groups.

3 Results

3.1 The influence of temperature on charred-mass production

Only needles and shrub leaves were greenish or brownish in colour at 250 $^{\circ}\text{C}$, but plant materials of all species were black with a typical charcoal appearance after burning at

300 and 350 $^{\circ}\text{C}$. A few fuel types (graminoid, *Sphagnum*, and some twigs) turned to ash at 400 $^{\circ}\text{C}$, whereas all other types of plant tissue became ash at 450 $^{\circ}\text{C}$ (File S1). Most of the charred materials remained intact and retained all of their morphological characteristics. However, samples burnt at higher temperatures tended to break easily during sample manipulation.

The average percentage of charred mass retained at 300 $^{\circ}\text{C}$ decreased as follows (Table 2; Fig. 1): brown moss and fern (50%) > shrub twigs (44%) > shrub leaf (46%) > forb leaf (42%) > needles (41%) > tree twigs (40%) > graminoid (29%) > *Sphagnum* (22%) > trunk wood (11%). This trend in mass loss was similar at all temperatures, although charcoal mass showed a marked decline from 38%–84% at 250 $^{\circ}\text{C}$ to 0.2%–23% at 400 $^{\circ}\text{C}$ across all fuel types. The charred mass of mixed-fuel samples at 300 $^{\circ}\text{C}$ was lowest for samples with high contents of graminoid and *Sphagnum* (33%–35%) and highest for samples with greater proportions of shrub material (38%).

3.2 Fuel-dependent variations in length, aspect ratio, and surface area

Graminoid charcoals burnt at 300 $^{\circ}\text{C}$ ($L/W = 11.5$; Fig. 2b, f; Table 2) were consistently more elongate than those of twigs (shrubs, 5.2; tree, 3.8), moss and fern stems (4.6), and leaves (2.7) (Table 2). Charred needles were more elongate (3.1) than those of leaves from heathland shrubs (2.4) and broadleaf trees (2.1) (Table 2). The Mann–Whitney test confirmed that (i) the median aspect ratio of graminoids was significantly different from those of all other fuel types ($p < 0.001$), (ii) those of all types of wood were different from those of leaves ($p < 0.001$) and moss (except at 350 $^{\circ}\text{C}$), and (iii) those of leaves were different from those of moss ($p < 0.001$; Table S2). The lengths (major axis, L) of charred particles from different fuel types, however, were less clearly differentiated (Fig. 3a, c; Files S2, S3). The surface area (A) varied greatly between individual taxa and fuel types; nevertheless, fragments of shrub leaves tended to be larger than all other fuel types (Fig. 3b, d; Table 2; Files S2, S4). The morphometrics of mixed-fuel samples showed that charcoal from samples with abundant graminoids and moss was more elongate (higher L/W) than charcoal from samples with higher proportions of shrubs, wood, and/or leaves (Fig. 2h). Similarly, the longest charcoal particles (higher L) were from samples with greater proportions of graminoids and moss (Fig. 3e), whereas the charcoals with the largest surface areas were from samples with more abundant shrubs and leaves (Fig. 3f). The aspect ratios and lengths of individual taxa and fuel types changed slightly with temperature, but the general trends were similar across all temperatures (Figs. 2, 3a, c; File S3). In contrast, relative surface areas varied more with temperature changes (Fig. 3b, d; File S4).

Table 2. Summary of the mean aspect ratio, length (µm), surface area (µm²), and mass retained (%) of charcoal produced in the muffle oven for individual plant species and fuel types from Siberia (SD denotes standard deviation). For the full taxa name, see Table 1. Please note that mean values are shown using bold font. [153](#)

Fuel types	Species	Aspect ratio at T (°C)				Length at T (°C)				Surface area at T (°C)				Mass retained at T (°C)				
		250	300	350	400	250	300	350	400	250	300	350	400	250	300	350	400	
Temperature	Graminoid	<i>Eriophorum</i>	7.2 ± 5.0	11.1 ± 6.4	5.8 ± 3.7	n/a	521 ± 545	797 ± 496	635 ± 74	n/a	37 665	42 744	51 820	n/a	42.6	29	3.6	2.9
		<i>Calamagrostis</i>	7.4 ± 4.6	12.9 ± 11.8	6.0 ± 3.8	n/a	620 ± 622	951 ± 712	440 ± 370	n/a	82 058	99 009	30 244	n/a	54.7	29.2	8.1	1.7
		<i>Carex</i>	7.4 ± 5.1	10.6 ± 7.0	8.3 ± 6.0	n/a	487 ± 499	841 ± 646	690 ± 709	n/a	32 165	82 947	51 982	n/a	50.9	29.5	7.9	1.2
		Mean	7.3 ± 0.1	11.5 ± 1.2	6.7 ± 1.4	n/a	543 ± 64	862 ± 79	588 ± 131	n/a	50 629	74 900	44 682	n/a	49.4	29.2	6.5	1.9
		<i>Equisetum</i>	4.8 ± 3.3	4.5 ± 2.8	3.1 ± 2.2	4.8 ± 3.1	506 ± 501	286 ± 233	655 ± 510	530 ± 424	71 381	25 955	166 741	75 098	54.4	49.4	31.0	21.4
Moss and ferns	<i>Polytrichum</i>	4.8 ± 3.1	4.2 ± 2.6	4.2 ± 2.6	4.7 ± 2.9	673 ± 665	461 ± 408	459 ± 476	572 ± 535	123 311	84 632	68 170	99 522	77.0	55.5	11.4	3.6	
	<i>Sphagnum</i>	3.4 ± 1.8	5.2 ± 6.2	3.2 ± 1.6	n/a	612 ± 574	524 ± 636	319 ± 217	n/a	109 185	77 224	24 724	n/a	38.3	21.7	8.3	0.2	
	Mean	4.3 ± 0.8	4.6 ± 0.5	3.5 ± 0.6	4.7 ± 0.1	598 ± 84	423 ± 123	477 ± 168	551 ± 29	97 346	62 739	86 545	87 310	56.6	42.2	16.6	8.4	
Wood (trunk)	<i>Pinus sylvestris</i>	2.0 ± 0.9	4.9 ± 2.8	2.5 ± 0.9	n/a	408 ± 347	391 ± 300	482 ± 384	n/a	105 057	57 028	97 673	n/a	63.5	11.1	1.8	1.4	
Wood (tree twig)	<i>Betula pendula</i>	2.8 ± 1.4	4.5 ± 3.1	2.0 ± 0.8	n/a	459 ± 402	361 ± 236	347 ± 85	n/a	120 539	37 630	54 180	n/a	50.8	40.2	10.9	0.3	
	<i>Picea abies</i>	2.3 ± 1.2	3.1 ± 1.9	2.5 ± 1.3	n/a	435 ± 371	439 ± 303	598 ± 575	n/a	92 767	92 107	199 556	n/a	56.5	40.1	16.8	3.4	
	<i>Pinus sibirica</i>	2.4 ± 1.3	3.1 ± 1.9	2.6 ± 1.3	n/a	450 ± 379	318 ± 248	427 ± 343	n/a	119 815	15 058	83 461	n/a	56.0	43.3	11.0	1.3	
	<i>Pinus sylvestris</i>	3.2 ± 1.7	3.5 ± 2.0	2.9 ± 1.7	2.9 ± 1.5	593 ± 558	379 ± 318	407 ± 295	407 ± 350	140 004	74 797	74 929	88 944	55.2	38.1	5.7	1.4	
	Mean	2.5 ± 0.4	3.8 ± 0.8	2.5 ± 0.3	2.9 ± 0.3	469 ± 72	377 ± 44	452 ± 95	407 ± 350	115 639	55 051	102 049	n/a	54.5	40.2	11.2	1.5	
Wood (shrub twig)	<i>Chamaedaphne</i>	3.5 ± 1.9	6.3 ± 3.5	3.7 ± 2.1	n/a	387 ± 340	347 ± 288	525 ± 528	521 ± 555	61 732	73 382	131 063	n/a	56.8	41.3	11.4	1.6	
	<i>Oxyccoccus</i>	3.8 ± 3.0	6.2 ± 3.5	4.7 ± 3.3	4.1 ± 2.3	674 ± 669	590 ± 419	591 ± 580	1053 ± 700	157 873	51 906	94 418	249 197	78.8	49.4	35.9	14.8	
	<i>Ledum</i>	4.4 ± 2.4	5.4 ± 2.8	2.9 ± 1.3	4.0 ± 2.7	333 ± 197	458 ± 288	342 ± 266	617 ± 580	57 191	56 836	254 696	131 860	56.6	52.5	15.6	0.9	
	<i>Vaccinium</i>	5.0 ± 3.1	3.0 ± 2.6	3.7 ± 2.5	n/a	461 ± 446	818 ± 714	441 ± 306	n/a	72 214	291 023	75 212	n/a	60.8	42.2	16.9	2.5	
	Mean	4.2 ± 0.7	5.2 ± 1.5	3.8 ± 0.7	4.0 ± 0.7	463 ± 150	553 ± 202	474 ± 107	730 ± 283	87 252	118 061	136 597	n/a	62.7	46	20	4.8	
Needles	<i>Picea abies</i>	2.6 ± 1.6	2.2 ± 1.1	2.3 ± 0.9	n/a	549 ± 535	342 ± 276	608 ± 692	n/a	118 375	86 728	242 364	n/a	67.2	52.3	26.2	4.9	
	<i>Pinus sibirica</i>	4.0 ± 2.3	3.6 ± 1.8	4.7 ± 2.9	n/a	606 ± 587	385 ± 292	432 ± 414	n/a	111 068	46 629	52 880	n/a	62.3	34.0	14.3	2.4	
	<i>Pinus sylvestris</i>	4.0 ± 2.5	3.7 ± 4.0	3.5 ± 2.9	n/a	690 ± 660	445 ± 376	492 ± 368	n/a	134 504	86 639	83 649	n/a	59.7	37.3	10.6	0.6	
	Mean	3.5 ± 0.8	3.1 ± 0.8	3.5 ± 0.1	n/a	613 ± 71	390 ± 52	510 ± 90	n/a	121 303	73 332	126 297	n/a	58.3	35.6	20.3	3.5	
Broadleaf (tree)	<i>Betula pendula</i>	2.1 ± 1.3	2.1 ± 0.9	2.0 ± 0.8	n/a	493 ± 498	335 ± 234	354 ± 185	n/a	156 591	67 692	57 934	n/a	58.3	35.6	20.3	3.5	
Broadleaf (shrub)	<i>Chamaedaphne</i>	2.4 ± 1.3	2.3 ± 1.7	1.8 ± 0.7	n/a	633 ± 493	347 ± 289	571 ± 395	n/a	176 620	73 382	216 473	n/a	61.8	44.7	27.2	4.3	
	<i>Oxyccoccus</i>	2.1 ± 0.9	2.3 ± 1.4	2.2 ± 1.0	1.9 ± 0.8	730 ± 486	590 ± 419	410 ± 343	260 ± 108	222 081	184 196	94 939	31 142	69.1	52.8	32.0	6.1	
	<i>Ledum</i>	2.3 ± 1.0	2.7 ± 1.4	2.7 ± 1.6	n/a	728 ± 698	393 ± 322	568 ± 586	n/a	281 751	67 913	219 788	n/a	84.5	47.4	31.9	8.3	
	<i>Vaccinium</i>	2.6 ± 2.0	2.1 ± 0.9	3.8 ± 2.8	2.1 ± 1.4	441 ± 334	414 ± 309	442 ± 304	401 ± 250	88 832	105 547	88 333	75 360	59.1	43.4	21.4	3.9	
	Mean	2.3 ± 0.1	2.4 ± 0.2	2.6 ± 0.8	2.0 ± 0.4	563 ± 99	385 ± 71	426 ± 101	330 ± 100	174 636	87 725	106 408	53 251	68.5	46.7	28	5.6	
Leaf (forb)	<i>Rubus</i>	1.9 ± 0.7	2.2 ± 1.1	2.1 ± 1.0	n/a	398 ± 355	354 ± 237	368 ± 315	n/a	99 109	79 877	88 927	n/a	49.8	40	35.2	12.1	
	<i>Cnidium</i>	2.3 ± 1.2	4.9 ± 2.6	2.6 ± 2.2	n/a	466 ± 384	372 ± 263	549 ± 598	n/a	108 610	34 207	176 828	n/a	50.3	41.1	37.3	23.6	
	<i>Polypodium</i>	2.1 ± 1.0	2.9 ± 2.0	2.5 ± 1.3	n/a	521 ± 399	464 ± 292	383 ± 284	n/a	155 561	106 241	60 473	n/a	61.4	50.6	29.4	18.2	
	Mean	2.1 ± 0.2	3.3 ± 1.4	2.4 ± 0.3	n/a	466 ± 61	418 ± 65	466 ± 117	n/a	132 085	70 224	118 650	n/a	56.6	44.3	33.6	17.6	

n/a – not applicable.

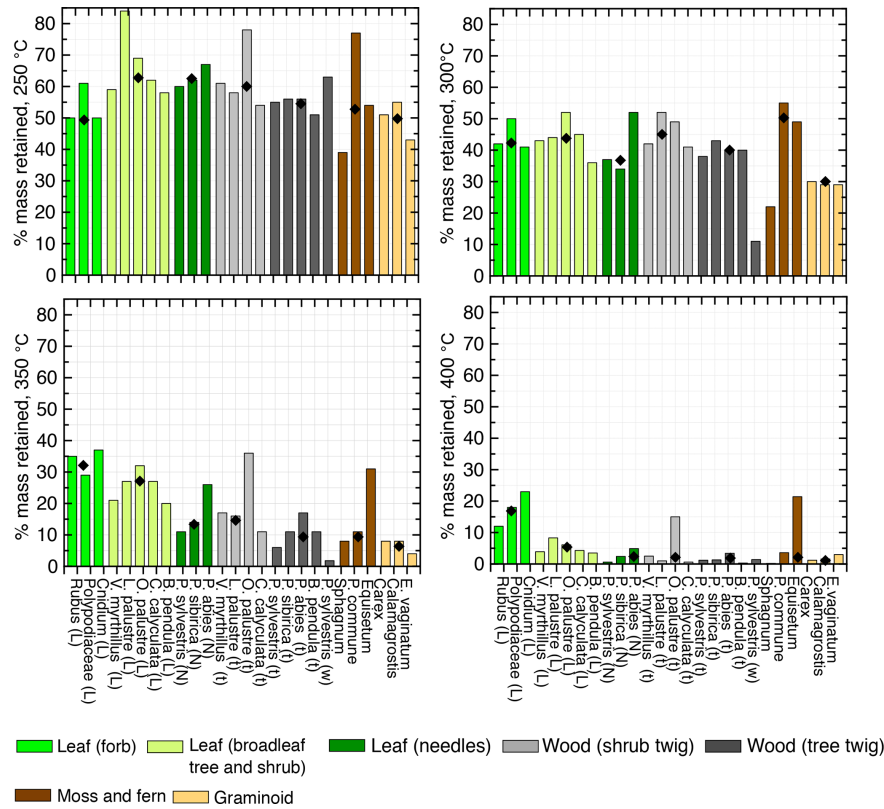


Figure 1. The percent of charred mass retained after burning known plant species from Siberia in a muffle oven at 250, 300, 350, and 400 °C. The abbreviations used in the figure are as follows: L – leaf, N – needles, t – twig, and w – wood. The median mass retained for similar fuel types (identified by the same colour) is reported as black diamonds.

3.3 Finer diagnostic features of the charcoal morphologies of various fuel types

3.3.1 Graminoid charcoal

Graminoid (*Carex*, *Calamagrostis*, and *Eriophorum vaginatum*) charred particles were consistently flat, rectangular, and elongated (Files S5a, S6a). They mostly broke parallel to the long axis when pressured, resulting in highly elongated pieces with straight margins. They can also appear as featureless long, thin filaments. Charcoal produced at higher temperatures (350 °C) often had more irregular, zigzag, or denticulate margins. The most commonly preserved surface features were rectangular epidermal cells or contained oval voids, reticulated or mesh patterns, and/or isolated veins.

3.3.2 Wood charcoal (trunk, tree twigs, and shrub twigs)

Wood charcoal pieces from a tree trunk (*Pinus sylvestris*) were blocky and quadrilateral with 90° corner angles (Files S5b, S6b). Wood charcoal from tree (*P. sylvestris*, *P. sibirica*, *Picea abies*, and *Betula pendula*) and shrub (Ericaceae) twigs showed both quadrilateral and polygonal shapes. The edges of both trunk and twig charcoal were

smooth, serrated, or denticulate, and surface textures were smooth, foliated, or striated (File S5b). Trunk charcoal of *P. sylvestris* showed rows of brown, open pits in the tracheid walls. Under the microscope, trunk charcoal fragments were shinier and darker than twig charcoals. Large charcoal pieces often broke parallel to the long axis, producing many tiny, elongated pieces (trunks) or pieces of various forms (twigs).

3.3.3 Leaf charcoal (needles, deciduous tree and shrub, forb, and fern)

Charred needle fragments were elongated and rectangular (corner angles of 90°; Files S5c, S6a). Their edges were smooth but became serrated and denticulate when broken. Surface features included visible venation and ridges. Charcoals from the leaves of deciduous trees (*Betula*), heathland shrubs (*Oxycoccus*, *Ledum*, *Chamaedaphne*, and *Vaccinium*), herbaceous plants (*Rubus*), and ferns (Polypodiaceae) were polygonal. Only those of *Cnidium* leaves were elongated, reflecting their needle shape. Edges were mostly undulate but were sometimes smooth or denticulate. Surface textures were generally smooth (featureless) but sometimes included visible venation and ridges. When broken, they showed voids, reticulated mesh patterns, and curly fibres. Birch leaves pro-

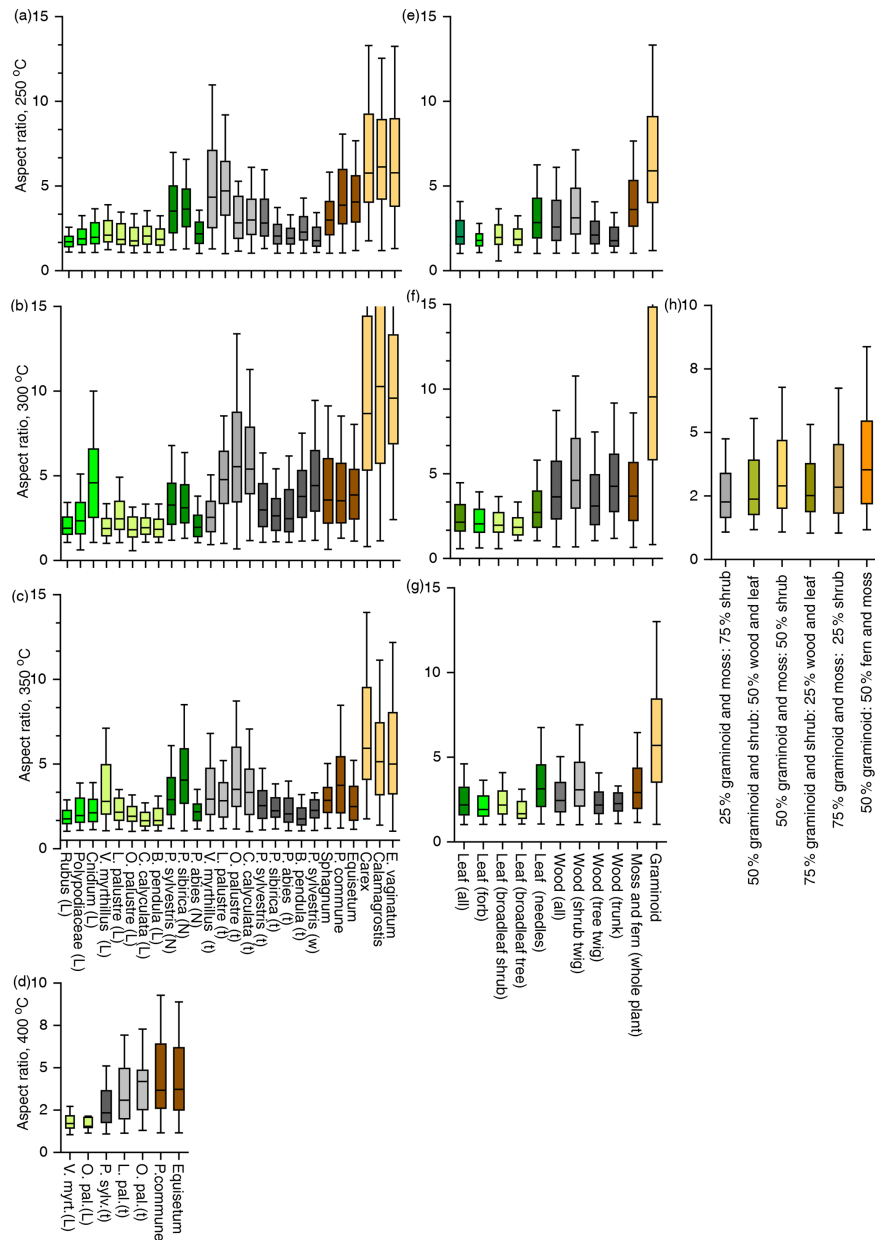


Figure 2. The median aspect ratios of charred particles from (a–d) the individual measurements burned at 250, 300, 350, and 400 °C respectively, and (e–g) fuel types at burning temperatures of 250, 300, and 350 °C respectively, as well as from (h) mixed-fuel samples burned at 300 °C. The fuel mixtures are arranged in order of increasing proportions of graminoids. Box plots represent the distribution of data as follows: the horizontal line in each box denotes the median, the upper quartile is the median value of the upper half of the data points, the lower quartile is the median value of the lower half of the data points, and whiskers represent the respective minimum and the maximum values. The abbreviations used in the figure are given in the caption of Fig. 1. The individual taxa (a–c) belonging to a fuel-type group (d–g) are indicated by the same colour.

duced visible charred veins with three branches diverging from a node. When pressured and broken, small leaf pieces had fracture lines radiating out at a variety of angles.

3.3.4 Moss and fern stems

Sphagnum produced two types of charcoal morphologies. Stems produced elongate particles with ramifications (scars) where leaves branched from the stem. Leaves preserved the anatomical features of the unburned leaves, i.e. a mesh-like appearance (Files S5a, S6a). *Polytrichum* produced several

Table 3. The mean aspect ratio, length, surface area, and the number of each charcoal morphotypes in the Holocene samples ranging from 185 to 6750 cal yr BP (35–303 cm) from Ulukh-Chayakh mire. The local to regional vegetation is represented by the percentages of the main pollen types, whereas the local vegetation is represented by the plant macrofossils (values in parentheses are presented as numbers except for the wood remains, which are presented as percentages).

Depth (cm)	35	84	85	172	248	268	303
Aspect ratio	3.2	3.0	3.0	4.0	11.1	4.3	2.8
Length (µm)	742	555	723	488	403	515	431
Surface (µm ²)	248.287	122.599	219.413	49.673	16.565	53.354	53.698
Charcoal morphologies (plant macrofossil)							
Wood	23 (6 %)	13 (5 %)	6 (5 %)	11 (15 %)	1 (0 %)	8 (0 %)	6 (0 %)
Leaf	11 (0)	7 (0)	3 (0)	2 (0)	0 (0)	4 (0)	4 (0)
Needle	0 (7)	1 (0)	0 (0)	0 (0)	0 (0)	0 (0)	0 (0)
Graminoid	21 (30)	9 (70)	1 (70)	11 (45)	4 (65)	19 (70)	3 (0)
<i>Equisetum</i>	15 (10)	3 (5)	1 (0)	0 (15)	0 (10)	5 (5)	0 (90)
Moss	10 (30)	0 (5)	0 (5)	1 (5)	1 (5)	3 (5)	1 (0)
Pollen (%)							
Trees	90	92	92	94	97	92	97
Shrub	1.1	3.4	3.4	3.5	0.2	0.5	0
Graminoid	5	6.3	6.3	3	13	8.6	9.5
<i>Equisetum</i>	0.5	3.4	3.4	1.2	6.7	9	18
Moss	0	0.2	0.2	0	0	0.3	0

charcoal per unit biomass and retained the greatest mass at higher temperatures from 50 %–84 % at 250 °C to 4 %–24 % at 400 °C (Fig. 1). The charred mass of mixed-fuel samples burnt at 300 °C also changed according to the dominant fuel type. Pereboom et al. (2020) burned plant tissue from similar taxa occurring in the Alaskan tundra in a muffle oven (at 500 °C) and likewise found that graminoids have a lower charred-mass retention (25 %–27 %) than shrubs (up to 33 %). However, they did not test the leaves and wood of shrubs separately and also did not investigate the effect of different temperatures on charred mass. Burning experiments on American forest steppe plants in a muffle oven (at 350 °C) and under open-flame conditions showed that the mass retention of grass and deciduous leaf charcoal decreased more rapidly with temperature compared with wood charcoal (Umbanhowar and McGrath, 1998), which is in partial agreement with the findings of this study. A calorimetric combustion study of various fuel types from mostly tropical plants found that the charred mass of wood, needles, and *Equisetum* was greater than that of other leaf types, due to the higher bulk densities and fuel load (Hudspeth et al., 2018).

Although oven experiments do not fully replicate the burn conditions of natural wildfires, these experimental findings have practical implications for charcoal-based fire reconstructions. First, fuel types with low charred-mass retention at higher temperatures are likely to be under-represented in the sedimentary charcoal record. Cyperaceae (sedges) are the most common graminoids in fens and meso- and eutrophic bogs worldwide, and *Eriophorum* (sedge) and *Sphag-*

num (moss) are common in oligotrophic bogs. These fuel types will turn to ash even in relatively low-intensity fires (< 300 °C) and, thus, may leave little or no trace of charcoal in sediments. Second, the woody biomass of typical heathland shrubs from oligotrophic bogs such as *Vaccinium*, *Chamaedaphne*, *Oxycoccus*, and *Ledum* as well as brown moss (*Polytrichum commune*), common in all boreal habitats, preserve almost half of their biomass when burnt at temperatures up to 300 °C, but their mass declines strongly (11 %–15 %) at higher temperatures (> 350 °C). This suggests that charcoal from these fuel types is likely to be preserved only when fires are of low to intermediate intensity. Third, the leaves of shrubs, forbs, and ferns as well as stems with leaves of *Equisetum* are more likely to persist as charcoal (27 %–38 %) after high-temperature fires and, thus, may contribute disproportionately to sedimentary charcoal. Mineral constituents can slow pyrolysis (thermal decomposition of plant material producing volatile products and a solid charred residue), and this may explain why *Equisetum* stems, with high silica content, produce more charcoal. Fuel with higher lignin content, such as wood, might also be expected to produce more charcoal than fuels higher in cellulose and hemicellulose, such as leaves (Yang et al., 2007). However, this did not appear to be the case in the current experiments where leaves retained a higher charred mass than wood with increasing burn temperature. This suggests that there is a need for further research on the quantitative relationship between temperature and charcoal mass retention for fuels with various structures, chemistry, and bulk density.

4.2 Fuel-dependent variability in charcoal morphometrics: implications for the reconstruction of fuel type and transportation by air and water

The consistency of the morphometrics of charred fragments between species in the same genus or family suggests that these measurements are useful for fuel-type identification. Graminoid charcoal particles are at least twice as elongated (6.7–11.5) as all other charcoal types and differ the most from leaf charcoal across all temperatures (Fig. 2; Table 2; File S7). Highly elongated and narrow graminoid charcoal is thought to reflect the occurrence of conspicuous veins parallel to the long axis (Umbanhowar and McGrath, 1998; Crawford and Belcher, 2014). Charred fragments of leaves (2.0–2.7 broadleaves; 3.1–3.5 needles) are also markedly more circular than those of other fuel types. However, there is some degree of overlap between the aspect ratios of woody twigs (2.5–5.2) and those of moss and fern stems (3.5–4.7; Table 2). In agreement with Crawford and Belcher (2014) and Umbanhowar and McGrath (1998), these experiments showed that smaller particles have a lower aspect ratio (i.e., more circular particles). Although larger charcoal fragments may be more suitable to categorise fuel type, there is no obvious threshold for determining what particle size should be used. Charcoal fragments from mixed-fuel samples preserve the aspect ratio of the dominant fuel type; particles with highest aspect ratios (3.5) were found in samples with greater proportions of graminoids and moss. Length and mean surface area do not appear to distinguish between fuel types reliably, except for the slight tendency for charred shrub leaf particles to be larger than those of all other fuel types (Fig. 3; File S4; Table 2). The larger shrub leaf fragments may be explained by the arrangement of leaf venation, with fragments breaking along the three branching veins that diverge from nodes (Umbanhowar and McGrath, 1998; Jensen et al., 2007). The measured aspect ratio of graminoids as well as shrub and forb leaves from this study are quite similar to those from the Alaskan Arctic, where graminoids (*Eriophorum vaginatum* and *Carex bigelowii*) show aspect ratios ranging from 5.46 to 8.09 (mean 6.77), and shrubs (*Ledum palustre*, *Salix pulchra*, *Betula nana*, *Rubus chamaemorus*, and *Vaccinium vitis-idaea*) show aspect ratios ranging from 2.09 to 2.50 (mean 2.42, Table 4; Pereboom et al., 2020). Considerably shorter graminoid particles (3.62) were obtained from American steppe forests (Umbanhowar and McGrath, 1998), although the aspect ratios obtained for leaves (1.91) and wood (2.13) were closer to those obtained in this study. Crawford and Belcher (2014) produced charcoal under laboratory conditions with an aspect ratio of 3.7 for graminoids, 2.23 for leaves, 1.97 for wood, and 2.8 for *Pinus sylvestris* needles (Table 4). Fossil charcoal assemblages from tropical African forests and grasslands were used to separate graminoids (aspect ratio < 2.0) from shrubs (> 2.0; Aleman et al., 2013). However, Daniau et al. (2013) interpreted an increase in the aspect ratio as an indication

of the increased proportion of burning of the grass fuel. Courtney-Mustaphi and Pisaric (2014a) also observed that burning monocotyledons from boreal Canada in the laboratory generally produced more elongated charcoal morphologies than other fuels. In term of surface area, Umbanhowar and McGrath (1998) show a surface area of 65.630 μm^2 (56.737 herein) for graminoids, 50.150 μm^2 (103.138 herein) for wood, and 64.946 μm^2 (versus 114.952 herein) for leaves, which are values comparable to Pereboom et al. (2020), who found little differentiation between average surface area for shrub (88.246 μm^2) and graminoid (87.474 μm^2) species. The present study suggests that the morphometric values are generally preserved for all fuel types over the range of temperatures explored, whereas Umbanhowar and McGrath (1998) found that burn temperature marginally reduced the aspect ratios of wood.

The combined results from this study and the published literature suggest that, despite some variability in morphometrics of charcoal assemblages from similar fuel types, the aspect ratio decreases from graminoids to wood and leaves. Differences in the aspect ratio might allow the distinction of graminoids from other fuel types in a consistent way. Although there is a wide range of individual measurements, the mean aspect ratios of the three graminoid species (6.7–11.5) suggests that a threshold aspect ratio of 6 could be used to discriminate graminoids. This threshold value appears to be most consistent for wetland graminoids (mean 6.77 for Arctic Alaska) but may be too high for graminoids from temperate grasslands (3.8–4.66; Table 4; File S7). Although there is also a good consistency in the aspect ratio of laboratory-produced wood (2.1–4.5) and leaf (2.0–3.5) charcoal particles across studies, these values overlap, suggesting that it is not possible to specify a threshold value at which charcoal particles are indicative of wood or leaves. Therefore, the use of charcoal morphologies in fuel-type identification requires the use of fine anatomical features (see Sect. 4.3) or validation from other sources, such as anthracological analysis as employed in archaeobotanical studies (Hubau et al., 2012, 2013, 2015; de Melo Júnior, 2017).

Particle shape affects the behaviour of charcoal during transportation by air (Clark and Hussey, 1996; Clark, 1988) and water (Nichols et al., 2000). Models, assuming a uniform spherical particle shape, and empirical data of transportation by fume indicate that the amount of charcoal particles is greatest near the fire source (Clark, 1998; Tinner et al., 2006; Higuera et al., 2007; Peters and Higuera, 2007). However, recent models accounting for different shapes, sizes, and densities of charcoal show that non-spherical particles have lower settling velocities than spherical particles and produce a spatially more extensive and heterogeneous particle-size distribution pattern – i.e., dispersal distances for spherical and aspherical particles greater than 150 μm could be up to 20 km apart (Vachula and Richter, 2018). Similarly, Clark and Hussey (1996) derived a velocity index for sedimentary charcoal particles and found that non-spherical particles have

Table 4. Comparative results of the aspect ratio from plant species analysed in this study with those from literature. “*Pinus sylvestris* (wood)” sums the mean aspect ratio of wood from trunk and twig; “Wood (total)” sums the mean aspect ratio of wood from trees and shrubs (trunk and twig); “Broadleaf” sums the mean aspect ratio of leaf from trees and shrubs, whereas “Leaf (total)” averages the mean aspect ratio of all leaf types.

Fuel type	250 °C	300 °C	350 °C	400 °C	500/550 °C	Open flame	References
Graminoid (boreal)	7.3	11.5	6.7	–	–	–	This study
Graminoid (Arctic)	–	–	–	–	6.7	–	Pereboom et al. (2020)
Graminoid (forest steppe)	–	–	3.6	–	–	4.8	Umbanhowar and McGrath (1998)
Graminoid (grass)	–	–	–	–	3.7	–	Crawford and Belcher (2014)
<i>Pinus sylvestris</i> (wood)	2.7	4.1	2.7	2.9	–	–	This study
<i>Pinus sylvestris</i> (wood)	–	–	–	–	2.8	–	Crawford and Belcher (2014)
Wood (total)	3.4	4.5	3.1	4.0	–	–	This study
Wood (forest steppe)	–	–	2.1	–	–	2.3	Umbanhowar and McGrath (1998)
Shrubs (wood and leaf)	–	–	–	–	2.4	–	Pereboom et al. (2020)
Broadleaf	2.2	2.2	2.3	2.0	–	–	This study
Needles	3.5	3.1	3.5	–	–	–	This study
Leaf (total)	2.5	2.7	2.6	2.0	–	–	This study
Leaf (forest steppe)	–	–	1.9	–	–	2.1	Umbanhowar and McGrath (1998)
Leaf	–	–	–	–	2.2	–	Crawford and Belcher (2014)

lower setting velocities and a higher residence time into the atmosphere than spherical particles. Based on these studies, it appears that non-spherical charcoal particles (elongated) such as those of graminoids, moss, and ferns are likely to have a more heterogeneous distribution and be deposited farther away from the origin of a fire than the rounder, polygonal leaf particles.

Erosion during hydrological transportation can also change the shape of buried (sedimentary) charcoal and can be an important consideration when interpreting charcoal morphometrics (Patterson et al., 1987; Nichols et al., 2000; Scott, 2010). Laboratory experiments simulating fluvial transportation found that the surface area of leaf charcoal decreases and circularity increases with transportation, whereas changes in the shape of woody particles is less evident with transportation, and grassy charcoal preserves a high aspect ratio during transportation (Crawford and Belcher, 2014). However, Nichols et al. (2000) found a slight rounding of sharp-angled edges of wood and a greater propensity for breakage of charcoal produced at higher temperatures, the latter of which was also found in this study. These findings give further support to the fact that the typical appearance of graminoids as elongated particles and of leaves as circular is preserved during transportation. Nevertheless, other studies using sedimentary charcoal records suggest that erosion during transport accounts for the rounding (degree angles are eroded) of robust charcoal types such as wood, whereas fragile pieces of leaves and grass may break (Vanni re et al., 2003; Courtney-Mustaphi and Pisaric, 2014b; Courtney Mustaphi et al., 2015). The differential transportation by air and the fragility of sedimentary charcoal morphotypes calls for investigations into the influence of particle shape on charcoal transportation and into strategies target-

ing coring locations for generating robust quantitative data for palaeo-fire interpretations.

4.3 Finer diagnostic features of the charcoal morphologies for fuel-type identification

Results from fine diagnostic features of charcoal particles show that these can be used to attribute charcoal particles to certain fuel types with some confidence. Apart from the extremely elongated shape that differentiates graminoid charred particles from all other fuel types, graminoids are further distinguished under both microscope and stereomicroscope by their flat appearance and breakage into thin filaments (Files S5a, S6a). Rectangular epidermal cells, reticulate meshes, and oval voids of former epidermal stomata are also good diagnostic features of graminoids (Grosse-Brauckman, 1974). The graminoid charcoals produced in this study are most similar to types C4, C6, D1, D2, and D3 described by Courtney-Mustaphi and Pisaric (2014a) and Enache and Cumming (2006). Comparative studies on graminoid charcoal originating from Poaceae (grass) and Cyperaceae (sedge) would further improve the identification of fuel types given the ecological differences of the two groups, with sedges growing in wet habitats and grass in drier habitats.

A distinct feature of woody charcoal is that they are layered with foliated or striated textures and break into many tiny particles when pressured (Files S5a, S6b). This is due to the abundance of fibres and xylem, which leads to charcoals splitting at various angles (Vaughan and Nichols, 1995). Additionally, conifer wood charcoal presents distinct rows of open pits in the tracheid walls (Schweingruber, 1978). Attempts to distinguish between charred trunk and twig particles were less successful, although charred trunk particles

are blockier. Foliated charred wood fragments also share appearance with moss and fern stems. These woody charcoals are most similar to types A1, B1, B2, and B3 (Courtney-Mustaphi and Pisaric, 2014a; Enache and Cumming, 2006).

Typical features of charred deciduous leaves are their polygonal shapes with surfaces characterised by void spaces or undulated surfaces (Files S5c, S6a). Netted venation is also sometimes visible, mostly with three branches diverging from a node. In contrast, conifer needles are elongated, often show ramification, and can have a wood-like appearance. The deciduous leaf charcoals found here are most similar to morphologies A2, A3, A4, A5, and A46, and conifer needle charcoals are most similar to morphologies C1, C2, and C3 (Courtney-Mustaphi and Pisaric, 2014a; Enache and Cumming, 2006).

Charred *Sphagnum* leaves preserve the meshed pattern of fresh plant material (Grosse-Brauckman 1972). Often, stems contain ramification, likely scars of former leaves (Files S5a, S6a). Both *Sphagnum* and *Polytrichum* charcoals present curvy fragments not seen in other fuel types. However, stems of *Sphagnum* and *Polytrichum* can be easily mistaken for shrub twigs. Burnt *Equisetum* can resemble graminoid charcoal. Charred moss is similar to morphologies C4 and C7 (Courtney-Mustaphi and Pisaric, 2014a; Enache and Cumming, 2006).

4.4 The morphometrics and morphologies of fossil charcoal particles: implications for fuel-type identification

Charcoal fragments from Holocene samples ranging from 6700 to 180 cal yr BP at the Ulukh-Chayakh mire preserved the aspect ratio of the dominant morphologies, i.e. particles with the highest aspect ratios (4–11) were found in samples with a greater proportion of graminoids, *Equisetum*, and moss (Table 3). Likewise, a greater surface area was found in samples with a higher number of leaves. Comparative results from fossil charcoal morphologies and morphometrics to those from pollen and plant macrofossils from the same depths show a partial agreement. For example, the pollen record indicates that the percentages of tree were > 90 % and the percentages of shrub were up to 3 % during the entire period, whereas the abundance of woody charcoal morphologies increased infrequently. This suggests that although there was a continuous source of woody fuel to burn, the production of wood charcoal from high-intensity fire only occurred occasionally. There is, however, a better agreement between samples with greater aspect ratios and morphologies of understorey vegetation (i.e. graminoids, *Equisetum*, and moss) and the proportion of these plants in the pollen and plant macrofossil records (Table 3). These findings are in line with the Siberian wildfire behaviour of predominantly low-intensity, surface fires, fuelled by graminoids, forbs, ferns, and mosses, or intermediate-intensity surface fires (shrubs) and only infrequently as high-intensity crown fires (Ander-

son, 1992). Another practical application of this finding is that the morphometrical and morphological characterisation of fossil charcoal is more representative of fuel type (what plant types were burning), compared with the pollen data and plant macrofossils that reflect plant types growing regionally and locally.

4.5 Applications for fuel- and fire-type reconstructions

The physical and chemical characteristics of fuel are key factors influencing ignition and fire propagation. The major chemical components of fuels are cellulose, hemicellulose, and lignin, and the minor components include terpenes, resins, and minerals (Planas and Pastor, 2014). Fuels rich in cellulose and hemicellulose (i.e. leaves) pyrolyse at a lower and narrow temperature range (200 and 400 °C), whereas those rich in lignin (i.e. wood) pyrolyse at a higher and wider range of temperatures (160–900 °C; Yang et al., 2007). Fuel types rich in terpene and resins (conifer wood, needles, and Ericaceae) burn faster and at higher temperatures, whereas those rich in mineral components (graminoids) burn less efficiently and at lower temperatures (200 °C) (Plana and Pastor, 2014). Fossil samples dominated by graminoid morphotypes show a high aspect ratio (4–11), which is in line with the elongated shape of graminoid charcoal found in burning experiments (> 6.7–11.5; Tables 2, 3). As graminoid charcoal typically preserves at lower temperatures, it likely suggests a graminoid fuel source and, therefore, a lower-intensity fire (Fig. 4). Fossil samples with abundant leaves and wood morphologies showed considerably lower aspect ratios (3–3.2), in agreement with values from laboratory-derived morphologies of leaves (2.1–3.5) and wood (2.0–5.2). Thus, shorter, and bulkier charcoal particles likely indicate the increased prevalence of leaves and wood as a fuel source (Figs. 2, 4). Because the morphometrical and morphological characteristics of leaves, and wood from trees and shrubs overlap, it is hard to distinguish between high-intensity surface fires, combusting living shrubs and dead wood and leaves, and high-intensity crown fires that have burnt living trees. Nevertheless, the fact that the past fires may have been of higher intensity at times of leaf and wood charcoal dominance than during the graminoid charcoal dominance is additionally suggested by the increased abundance of morphologies of *Equisetum* and *Polytrichum*, which are taxa found to remain as charcoal after burning at high temperature.

In summary, the consistency of results from this study with those from the literature on various vegetation types (boreal, temperate, and tropical woodlands; and grasslands) suggests the potential of charcoal morphometrics and morphologies in palaeoecology. For example, the expansion of open habitats during deep geological times or with human impact, the recession of latitudinal and elevational treelines, or the predominant occurrence of surface fires is likely to be reflected in an increase in aspect ratio and graminoid mor-

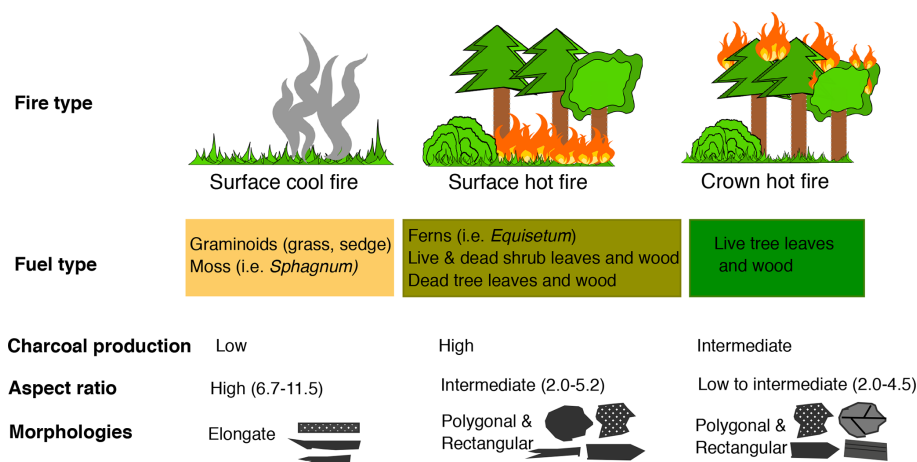


Figure 4. Schematic representation of fire types, and the potential link with fuel types burnt and predominant charcoal morphometrics (aspect ratio) and morphologies as well as charcoal production.

phologies relative to total biomass burning. Conversely, the closing up of the forests, shrub encroachment, or the predominance of crown fires may show itself in a decreased aspect ratio of particles and increased bulky morphologies derived from leaves and wood. Results could also provide forest managers with the range of fire types that key boreal species experienced in the past, which is useful when aiming to make choices for prescribed burning to remove fuel and prevent large fires or select species that will be fit to cope with future fire regimes. Answering all of these questions, however, will require further investigations in order to relate the proportion of charcoal morphotypes to the quantity of biomass and extend the morphometric and morphological characterisation to key species of interest.

5 Conclusions and recommendations

This study presents the first results on the morphometry and other diagnostic features of charred particles produced in the laboratory from seven fuel types comprising 17 plant species from boreal Siberia and demonstrates the applicability of these experiments to interpreting fossil charcoal records. The use of a higher number of fuel types from species with broad geographical coverage combined with an exploration of various combustion temperatures improves the link between charcoal morphologies, fuel types, and fire characteristics. Results show a distinct effect of temperature on fuel types, suggesting that species with low mass retention (graminoid, *Sphagnum*, and trunk wood) during high fire temperature are likely to be under-represented in the fossil charcoal record. The aspect ratio was the strongest indicator of fuel type. Graminoid charcoal particles are more elongate (6.7–11.5) than all other fuel types, with a threshold above 6 that may be indicative of wetland graminoids; leaves are the shortest and bulkiest (2.1–3.5); and twigs and wood are intermedi-

ate (2.0–5.2). Other diagnostic features can be used to separate wood, graminoids, and leaves, but not to make further distinctions within these fuel types. Distinct particle shape may influence charcoal transportation, with elongated particles (graminoids, moss, and ferns) potentially having a more heterogeneous distribution and being deposited farther away from the origin of a fire than the rounder, polygonal particles (leaf).

Despite these limitations, the combined use of particle aspect ratio and charred morphotypes should allow more robust interpretations of changes in fuel source and fire type from charcoal records. Future efforts to determine fuel sources based on analyses of small charcoal fragments will require (i) a more detailed examination of plant anatomy; (ii) investigation of the proportion of particular charcoal morphotype to the quantity of biomass; (iii) quantification of the relationship between the chemical composition of fuels, combustion temperature, and charcoal production; (iv) determination of the influence of particle shape on differential transportation and fragility; and (v) the use of image-recognition software to collect data on charcoal characteristics such as roundedness, reflectance, and others features that could improve the estimation of fire temperature and erosion during transportation.

Appendix A: The watershed algorithm used to calculate morphometrics of charred particles

The algorithm for automatic detection of morphometrics is based on functions from the “skimage” Python module (watershed algorithm). First, the picture is converted to a greyscale image. A Sobel gradient of the picture is then calculated, which results in an elevation map. To use the watershed algorithm to detect the charcoal particles, a map of markers in the grey picture with grey values higher than 140 is then created. These are the starting points of the watershed region fill algorithm. Finally, any holes in the watershed regions are filled with the help of a binary fill method (Soille and Vincent, 1990). The detected particles are subject to the calculation of morphometrics such as surface area and lengths along the major and minor axis via supported functions. Particles with a major axis length less than 150 μm are excluded from these calculations. The pixel area is calibrated at the micrometre scale, and the results are scaled accordingly.

Data availability. A limited amount of burnt plant material can be made available from the author upon reasonable request.

Supplement. The supplement related to this article is available online at: <https://doi.org/10.5194/bg-18-1-2021-supplement>.

5 *Competing interests.* The author declares that there is no conflict of interest.

Special issue statement. This article is part of the special issue “The role of fire in the Earth system: understanding interactions with the land, atmosphere, and society (ESD/ACP/BG/GMD/NHESS inter-journal SI)”. It is a result of the EGU General Assembly 2020, 3–8 May 2020.

Disclaimer. Publisher’s note: Copernicus Publications remains neutral with regard to jurisdictional claims in published maps and institutional affiliations.

15 *Acknowledgements.* I would like to thank Markus Rosenstihl for help with developing the code for the automatic detection of charred particles and drawing the pictograms in Fig. 4, Dagmar Fritzsich for initial brainstorming on the burning experiments, Doris Schneider for help with burning plant material in the muffle oven, and Sergey Kirpotin for help with the identification of plant species in the field. Simon Hutchinson and Mirjam Pfeiffer provided some of the linguistic suggestions.

Financial support. This research has been supported by the Deutsche Forschungsgemeinschaft (grant no. FE_1096/6).

25 This open-access publication was funded by the Goethe University Frankfurt.

Review statement. This paper was edited by Sandy Harrison and reviewed by three anonymous referees.

30 References

- Anderson, R. C.: The eastern prairie-forest transition – an overview, in: Proceedings of the eighth North American Prairie Conference, edited by: Ballard Jr., H. E., Brewer, L. S., and Fox, C., Western Michigan University, Kalamazoo, Michigan, 86–92, 1992.
- 35 Aleman, J. C., Blarquez, O., Bentaleb, I., Bonté, P., Brossier B., Carcaillet, C., Gond, V., Gourlet-Fleury, S., Kpolita, A., Lefèvre, I., and Oslisly, R.: Tracking landcover changes with sedimentary charcoal in the Afrotropics, *Holocene*, 23, 1853–1862, <https://doi.org/10.1177/0959683613508159>, 2013.

- Belcher, C. M., Collinson, M. E., and Scott, A. C.: Constraints on the thermal energy released from the Chicxulub impactor: new evidence from multi-method charcoal analysis, *J. Geol. Soc.*, 162, 591–602, <https://doi.org/10.1144/0016-764904-104>, 2005.
- Belcher, C. M., Hadden, R. M., Rein, G., Morgan, J. V., Artemieva, N., and Goldin, T.: An experimental assessment of the ignition of forest fuels by the thermal pulse generated by the Cretaceous–Palaeogene impact at Chicxulub, *J. Geol. Soc.*, 172, 175–185, <https://doi.org/10.1144/jgs2014-082>, 2015.
- Clark, J. S.: Particle motion and the theory of charcoal analysis: source area, transport, deposition, and sampling, *Quaternary Res.*, 30, 67–80, [https://doi.org/10.1016/0033-5894\(88\)90088-9](https://doi.org/10.1016/0033-5894(88)90088-9), 1988.
- Clark, J. S. and Hussey, T. C.: Estimating the mass flux of charcoal from sedimentary records: effects of particle size, morphology, and orientation, *Holocene*, 6, 129–44, <https://doi.org/10.1177/095968369600600201>, 1996.
- Courtney-Mustaphi, C. J. and Pisaric, M. F. J.: Forest vegetation change and disturbance interactions over the past 7500 years at Sasquatch Lake, Columbia Mountains, western Canada, *Quaternary Int.*, 488, 95–106, <https://doi.org/10.1016/j.quaint.2017.03.045>, 2018.
- Courtney-Mustaphi, C. J. and Pisaric, M. F.: A classification for macroscopic charcoal morphologies found in Holocene lacustrine sediments, *Prog. Phys. Geogr.*, 38, 734–754, <https://doi.org/10.1177/0309133314548886>, 2014a.
- Courtney-Mustaphi, C. J. and Pisaric, M. F. J.: Holocene climate-fire-vegetation interactions at a subalpine watershed in southeastern British Columbia, Canada, *Quaternary Res.*, 81, 228–239, <https://doi.org/10.1016/j.yqres.2013.12.002>, 2014b.
- Courtney Mustaphi, C. J., Davis, E. L., Perreault, J. T., and Pisaric, M. F. J.: Spatial variability of recent macroscopic charcoal deposition in a small montane lake and implications for reconstruction of watershed-scale fire regimes, *J. Paleolimnol.*, 54, 71–86, <https://doi.org/10.1007/s10933-015-9838-2>, 2015.
- Crawford, A. J. and Belcher, C. M.: Charcoal morphometry for paleoecological analysis: the effects of fuel type and transportation on morphological parameters, *Appl. Plant Sci.*, 2, 1400004, <https://doi.org/10.3732/apps.1400004>, 2014.
- Daniau, A.-L., Gofii, M. F. S., Martinez, P., Urrego, D. H., Bout-Roumazelles, V., Desprat, S., and Marlon, J. R.: Orbital-scale climate forcing of grassland burning in southern Africa, *P. Natl. Acad. Sci., USA*, 110, 5069–5073, <https://doi.org/10.1073/pnas.1214292110>, 2013.
- de Melo Júnior, J. C. F.: A new archaeobotanical protocol for collecting concentrated wood charcoal from archaeological bonfire sites, *International Journal of Development Research*, 7, 14241–14247, 2017.
- Enache, M. D. and Cumming, B. F.: Tracking recorded fires using charcoal morphology from the sedimentary sequence of Prosser Lake, British Columbia (Canada), *Quaternary Res.*, 65, 282–292, <https://doi.org/10.1016/j.yqres.2005.09.003>, 2006.
- Enache, M. D. and Cumming, B. F.: Charcoal morphotypes in lake sediments from British Columbia (Canada): an assessment of their utility for the reconstruction of past fire and precipitation, *J. Paleolimnol.*, 38, 347–363, <https://doi.org/10.1007/s10933-006-9084-8>, 2007.
- Feurdean, A. and Vasiliev, I.: The contribution of fire to the late Miocene spread of grasslands in eastern Eurasia (Black Sea re-

- gion), *Sci. Rep.-UK*, 9, 1–7, <https://doi.org/10.1038/s41598-019-43094-w>, 2019.
- Feurdean, A., Veski, S., Florescu, G., Vanni re, B., Pfeiffer, M., O'Hara, R. B., Stivrins, N., Amon, L., Heinsalu, A., Vassiljev, J., and Hickler, T.: Broadleaf deciduous forest counterbalanced the direct effect of climate on Holocene fire regime in hemiboreal/boreal region (NE Europe), *Quaternary Sci. Rev.*, 169, 378–390, <https://doi.org/10.1016/j.quascirev.2017.05.024>, 2017.
- Feurdean, A., Tonkov, S., Pfeiffer, M., Panait, A., Warren, D., Vanni re, B., and Marinova, M.: Fire frequency and intensity associated with functional traits of dominant forest type in the Balkans during the Holocene, *Eur. J. Forest Res.*, 138, 1049–1066, <https://doi.org/10.1007/s10342-019-01223-0>, 2019.
- Feurdean, A., Florescu, G., Tan au, I., Vanni re, B., Diaconu, A. C., Pfeiffer, M., Warren, D., Hutchinson, S. M., Gorina, N., Ga ka, M., and Kirpotin, S.: Recent fire regime in the southern boreal forests of western Siberia is unprecedented in the last five millennia, *Quaternary Sci. Rev.*, 244, 106495, <https://doi.org/10.1016/j.quascirev.2020.106495>, 2020.
- Goldammer, J. G. and Furyaev, V. V. (Eds.): *Fire in Ecosystems of Boreal Eurasia*, Springer, Dordrecht, Germany, 1996.
- Grosse-Brauckmann, G.: *Über pflanzliche Makrofossilien mitteleurop ischer Torfe*, TELMA, Band 4, 51–117, Hannover, 1974.
- Hawthorne, D., Mustaphi, C. J. C., Aleman, J. C., Blarquez, O., Colombaroli, D., Daniau, A. L., Marlon, J. R., Power, M., Vanni re, B., Han, Y., and Hantson, S.: Global Modern Charcoal Dataset (GMCD): A tool for exploring proxy-fire linkages and spatial patterns of biomass burning, *Quaternary Int.*, 488, 3–17, <https://doi.org/10.1016/j.quaint.2017.03.046>, 2018.
- Higuera, P. E., Peters, M. E., Brubaker, L. B., and Gavin, D. G.: Understanding the origin and analysis of sediment-charcoal records with a simulation model, *Quaternary Sci. Rev.*, 26, 1790–1809, <https://doi.org/10.1016/j.quascirev.2007.03.010>, 2007.
- Hubau, W., Van den Bulcke, J., Mees, F., Van Acker, J., and Beeckman, H.: Charcoal identification in species rich biomes: a protocol for Central Africa optimised for the Mayumbe forest, *Rev. Palaeobot. Palynol.*, 171, 164–178, <https://doi.org/10.1016/j.revpalbo.2011.11.002>, 2012.
- Hubau, W., Van den Bulcke, J., Kitin, P., Brabant, L., Van Acker, J., and Beeckman, H.: Complementary imaging techniques for charcoal examination and identification, *IAWA J.*, 34, 147–168, <https://doi.org/10.1163/22941932-00000013>, 2013.
- Hubau, W., Van den Bulcke, J., Van Acker, J., and Beeckman, H.: Charcoal-inferred Holocene fire and vegetation history linked to drought periods in the Democratic Republic of Congo, *Glob. Change Biol.*, 21, 2296–2308, <https://doi.org/10.1111/gcb.12844>, 2015.
- Hudspith, V. A., Hadden, R. M., Bartlett, A. I., and Belcher, C. M.: Does fuel type influence the amount of charcoal produced in wildfires? Implications for the fossil record, *Palaeontology*, 61, 159–171, <https://doi.org/10.1111/pala.12341>, 2018.
- Jensen, K., Lynch, E., Calcote, R., and Hotchkiss, S. C.: Interpretation of charcoal morphotypes in sediments from Ferry Lake, Wisconsin, USA: do different plant fuel sources produce distinctive charcoal morphotypes?, *Holocene*, 17, 907–915, <https://doi.org/10.1177/0959683607082405>, 2007.
- Jones, M. W., Smith, A., Betts, R., Canadel, J. G., Prentice, I. C., and Le Qu er , C.: Climate change increases the risk of wildfires, <https://sciencebrief.org/briefs/wildfires> (last access: 19 June 2021), 2020.
- Leys, B., Brewer, S. C., McConaghy, S., Mueller, J., and McLaughlan, K. K.: Fire history reconstruction in grassland ecosystems: amount of charcoal reflects local area burned, *Environ. Res. Lett.*, 10, 114009, <https://doi.org/10.1088/1748-9326/10/11/114009>, 2015.
- MacDonald, G. M., Larsen, C. P. S., Szeicz, J. M., and Moser, K. A.: The reconstruction of boreal forest fire history from lake sediments: a comparison of charcoal, pollen, sedimentological, and geochemical indices, *Quaternary Sci. Rev.*, 10, 53–71, [https://doi.org/10.1016/0277-3791\(91\)90030-X](https://doi.org/10.1016/0277-3791(91)90030-X), 1991.
- Marlon, J. R., Kelly, R., Daniau, A.-L., Vanni re, B., Power, M. J., Bartlein, P., Higuera, P., Blarquez, O., Brewer, S., Br ucher, T., Feurdean, A., Romera, G. G., Iglesias, V., Maezumi, S. Y., Magi, B., Courtney Mustaphi, C. J., and Zhihai, T.: Reconstructions of biomass burning from sediment-charcoal records to improve data–model comparisons, *Biogeosciences*, 13, 3225–3244, <https://doi.org/10.5194/bg-13-3225-2016>, 2016.
- Moritz, M. A., Batllori, E., Bradstock, R. A., Gill, A. M., Handmer, J., Hessburg, P. F., Leonard, J., McCaffrey, S., Odion, D. C., Schoennagel, T., and Syphard, A. D.: Learning to coexist with wildfire, *Nature*, 515, 58–66, <https://doi.org/10.1038/nature13946>, 2014.
- Nichols, G. J., Cripps, J. A., Collinson, M. E., and Scott, A. S.: Experiments in waterlogging and sedimentology of charcoal: results and implications, *Palaeogeogr. Palaeoclimatol.*, 164, 43–56, [https://doi.org/10.1016/S0031-0182\(00\)00174-7](https://doi.org/10.1016/S0031-0182(00)00174-7), 2000.
- Orvis, K. H., Lane, C. S., and Horn, S. P.: Laboratory production of vouchered reference charcoal from small wood samples and non-woody plant tissues, *Palynology*, 29, 1–11, <https://www.jstor.org/stable/3687800> (last access: 21 June 2021), 2005.
- Patterson III, W. A., Edwards, K. J., and Maguire, D. J.: Microscopic charcoal as an indicator of fire, *Quaternary Sci. Rev.*, 6, 3–23, 1987.
- Pereboom, E. M., Vachula, R. S., Huang, Y., and Russell, J.: The morphology of experimentally produced charcoal distinguishes fuel types in the Arctic tundra, *Holocene*, 7, 1–6, <https://doi.org/10.1177/0959683620908629>, 2020.
- Peters, M. and Higuera, P.: Quantifying the source area of macroscopic charcoal with a particle dispersal model, *Quaternary Res.*, 67, 304–310, <https://doi.org/10.1016/j.yqres.2006.10.004>, 2007.
- Planas, E. and Pastor, E.: Wildfire behaviour and danger rating, in: *Fire phenomena and the Earth system: an interdisciplinary guide to fire science*, edited by: Belcher, C., 53–76, <https://doi.org/10.1002/9781118529539>, John Wiley & Sons, Ltd., 2014.
- Prince, T. J., Pisaric, M. F., and Turner, K. W.: Postglacial reconstruction of fire history using sedimentary charcoal and pollen from a small lake in southwest Yukon Territory, Canada, *Front. Ecol. Evol.*, 6, 209, <https://doi.org/10.3389/fevo.2018.00209>, 2018.
- Rein, G.: Smoldering fire and natural hazard, in: *Fire phenomena and the Earth system: an interdisciplinary guide to fire science*, edited by: Belcher, C., 15–34, <https://doi.org/10.1002/9781118529539>, John Wiley & Sons, Ltd, 2014.
- Schweingruber, F. H.: *Mikroskopische Holzanatomie Formenspektren mitteleurop ischer Stamm- und Zweigh olzer zur Bestimmung*

- mung von rezentem und subfossilem, Zürcher AG, 6301, Zug, 1978.
- Scott, A. C.: Charcoal recognition, taphonomy and uses in palaeoenvironmental analysis, *Palaeogeogr. Palaeoclimatol., 291*, 11–39, <https://doi.org/10.1016/j.palaeo.2009.12.012>, 2010.
- Soille, P. and Vincent, L. M.: Determining watersheds in digital pictures via flooding simulations, *Proc. SPIE*, 1360, 240–250, <https://doi.org/10.1117/12.242111>, 1990.
- Tinner, W., Hofstetter, S., Zeuglin, F., Conedera, M., Wohlgemuth, T., Zimmermann, L., and Zweifel, R.: Long-distance transport of macroscopic charcoal by an intensive crown fire in the Swiss Alps-implications for fire history reconstruction, *Holocene*, 16, 287–292, 2006.
- Umbanhowar, C. E. and McGrath, M. J.: Experimental production and analysis of microscopic charcoal from wood, leaves and grasses, *Holocene*, 8, 341–346, <https://doi.org/10.1191/095968398666496051>, 1998.
- Unkelbach, J., Dulamsuren, C., Punsalpaamuu, G., Saindovdon, D., and Behling, H.: Late Holocene vegetation, climate, human and fire history of the forest-steppe-ecosystem inferred from core G2-A in the “Altai Tavan Bogd” conservation area in Mongolia, *Veget. Hist. Archaeobot.*, 27, 665–677, <https://doi.org/10.1007/s00334-017-0664-5>, 2018.
- Vachula, R. S. and Richter, N.: Informing sedimentary charcoal-based fire reconstructions with a kinematic transport model, *Holocene*, 28, 173–178, <https://doi.org/10.1177/0959683617715624>, 2018.
- Vannière, B., Bossuet, G., Walter-Simonnet, A.V., Gauthier, E., Barral, P., Petit, C., Buatier, M., and Daubigny, A.: Land use change, soil erosion and alluvial dynamic in the lower Doubs Valley over the 1st millennium AD (Neublans, Jura, France), *J. Archaeol. Sci.*, 30, 1283–1299, 2003.
- Vaughan, A. and Nichols, G.: Controls on the deposition of charcoal: implications for sedimentary accumulations of fusain, *J. Sediment. Res.*, 65, 130–135, <https://doi.org/10.1306/D426804A-2B26-11D7-8648000102C1865D>, 1995.
- Walsh, P. M. and Li, T.: Fragmentation and attrition of coal char particles undergoing collisions during combustion at temperatures from 900–1100 K, *Combust. Flame*, 99, 749–757, [https://doi.org/10.1016/0010-2180\(94\)90070-1](https://doi.org/10.1016/0010-2180(94)90070-1), 1994.
- Walsh, M. K., Whitlock, C., and Bartlein, P. J.: A 14,300-year-long record of fire–vegetation–climate linkages at Battle Ground Lake, southwestern Washington, *Quaternary Res.*, 70, 251–264, <https://doi.org/10.1016/j.yqres.2008.05.002>, 2008.
- Ward, D. E. and Hardy, C. C.: Smoke emissions from wildland fires, *Environ. Int.*, 17, 117–134, 1991.
- Yang, H., Yan, R., Chen, H., Lee, D. H., and Zheng, C.: Characteristics of hemicellulose, cellulose and lignin pyrolysis, *Fuel*, 86, 1781–1788, <https://doi.org/10.1016/j.fuel.2006.12.013>, 2007.

Remarks from the language copy-editor

- CE1** Please confirm that the sentence is now correct.
- CE2** Please confirm that the sentence is now correct.
- CE3** Did you want something else changed here? “dominated” was underlined in the proofreading PDF. Please check.

Remarks from the typesetter

- TS1** Not mentioned in the reference list. Please add a reference to the reference list, even if the article is still in preparation. The addition “in preparation” should be added to the reference, not to the citation.
- TS2** Please give an explanation of why this needs to be changed. We have to ask the handling editor for approval. Thank you.
- TS3** The numbers in the tables have not yet been corrected. To ensure a transparent review process, I will have to ask the editor for approval. Could you please provide a short explanation regarding the requested changes in this table? Thank you very much in advance.
- TS4** Please see previous remark regarding editor approval.